Nanoscale

Accepted Manuscript

This article can be cited before page numbers have been issued, to do this please use: J. Yang, S. Kwak, S. Jeon, E. Lee, J. Ju, H. Kim, Y. Lee and J. Kim, *Nanoscale*, 2016, DOI: 10.1039/C6NR02815B.

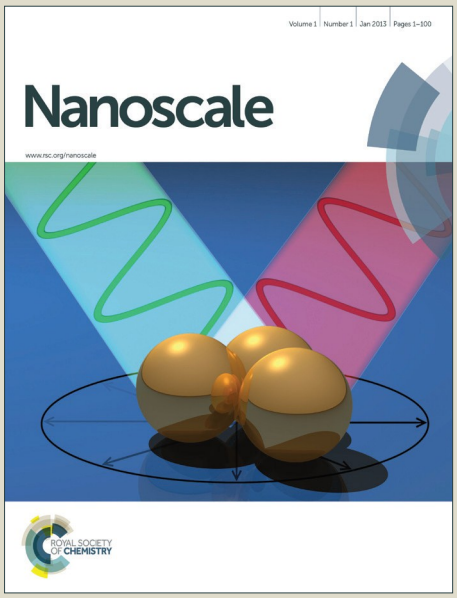

This is an *Accepted Manuscript*, which has been through the Royal Society of Chemistry peer review process and has been accepted for publication.

Accepted Manuscripts are published online shortly after acceptance, before technical editing, formatting and proof reading. Using this free service, authors can make their results available to the community, in citable form, before we publish the edited article. We will replace this *Accepted Manuscript* with the edited and formatted *Advance Article* as soon as it is available.

You can find more information about *Accepted Manuscripts* in the Information for Authors.

Please note that technical editing may introduce minor changes to the text and/or graphics, which may alter content. The journal's standard Terms & Conditions and the Ethical guidelines still apply. In no event shall the Royal Society of Chemistry be held responsible for any errors or omissions in this *Accepted Manuscript* or any consequences arising from the use of any information it contains.

ROYAL SOCIETY OF CHEMISTRY

www.rsc.org/nanoscale

View Article Online
DOI: 10.1039/C6NR02815B

Nanoscale

Paper

Proteolytic Disassembly of Peptide-mediated Graphene Oxide Assemblies for Turn-on Fluorescence Sensing of Proteases

Received 00th January 20xx,
Accepted 00th January 20xx

DOI: 10.1039/x0xx00000x

www.rsc.org/

Jin-Kyoung Yang[†,a], Seon-Yeong Kwak[†,b,c], Su-Ji Jeon[b], Eunjin Lee[a], Jong-Min Ju[b], Hye-In Kim[b], Yoon-Sik Lee[a,*], and Jong-Ho Kim[b,*]

Molecule-induced assembly of nanomaterials can alter their unique chemical and physical properties, which can be a promising approach for sensing. Herein, we demonstrate an optical 'turn-on' biosensor for the detection of matrix metalloproteinase-2 (MMP-2), fabricated by means of peptide-induced assembly of fluorescent graphene oxide (GO). Functionalization of GO with a peptide substrate for MMP-2 bearing a thiol group lead to its self-assembly via disulfide bonding, accompanied by self-quenching of GO's strong fluorescence. This peptide-induced GO assembly is then disassembled by proteolytic cleavage in the presence of MMP-2, thereby restoring the level of self-quenched GO fluorescence. With this approach, we are able to detect MMP-2 and to investigate the kinetic parameters of MMP-2 activity. The GO-peptide assembly is successfully applied to the selective and sensitive detection of MMP-2 secreted by living cells, human hepatocytes HepG2, at the concentration of 2 ng/mL.

1. Introduction

Molecule-induced assembly of nanomaterials has emerged as an effective strategy for manipulating their sizes, shapes and interparticle interactions, which can alter their unique chemical and physical properties.[1, 2] Fluorescent nanomaterials have been widely used as building blocks in molecule-induced assembly to modulate their optical properties.[3, 4] Fluorescent nanomaterials, when assembled, often show changes in their emission intensities and/or wavelengths, which can be subsequently restored to their original state by disassembly.[5-8] In particular, self-quenching driven by self-assembly of the fluorescent nanomaterials can be utilized as an effective principle for designing fluorescence sensors to detect target molecules, because interaction with the specific target molecules triggers the restoration of self-quenched fluorescence of the nanomaterials.[5, 7, 9] The self-quenching approach does not require any quencher molecules that are essential in fluorescence resonance energy transfer (FRET) sensors, and thus it allows simple and rapid detection with high signal-to-background ratio.[10-12]

Graphene oxide (GO), which is an oxidized form of graphene, is a new class of fluorescent nanomaterial. It emits strong fluorescence based on the recombination of electron-hole pairs localized within a small sp^2 carbon domain embedded in a sp^3 matrix.[13-17] The fluorescence of GO can easily be tuned to the visible and near-infrared range of the electromagnetic spectrum by controlling the extent of oxidation.[14, 18, 19] In addition, GO fluorescence has shown exceptional stability against photobleaching compared to that of organic fluorescent dyes.[20] Due to these excellent optical properties, GO fluorescence has recently been used as a signal transduction tool in biosensors.[21-24] However, GO fluorescence-based sensors still remain at an early stage of development while GO has been mostly exploited as a universal quencher in various FRET bioassay systems rather than as a fluorophore.[25-28] The self-quenching mechanism accompanied by molecule-induced assembly of nanomaterials has not yet been applied to the design of GO fluorescence biosensors for selective detection of biological molecules. Therefore, it is of great interest to develop self-quenching-based biosensors operating by means of an assembly of fluorescent GO for selective recognition of proteins.

Matrix metalloproteinases (MMPs) are endopeptidases capable of breaking down the extracellular matrix (ECM) to control cell behaviors in regular biological processes. MMPs are believed to be involved in cancer biology,[29] including cancer cell growth, differentiation, apoptosis, migration, invasion, and immune surveillance.[30] Among MMPs family, MMP-2 has been considered to be a putative tumor marker for clinical applications, since it is known to be closely associated with the metastasis of malignant cells.[31, 32] To date, several strategies have been reported for the detection of MMP-2, such as zymography[33], enzyme-linked immunosorbent assay (ELISA)[34], and activity assays[35]. However, these methods often require multiple reaction steps, making them time-consuming, laborious, and complex.[36] Hence, simpler and more efficient approaches continue to be explored for the selective detection

[a] School of Chemical and Biological Engineering, Seoul National University, Seoul 151-744, Republic of Korea
[b] Department of Chemical Engineering, Hanyang University, Ansan 426-791, Republic of Korea
[c] Current address: Department of Chemical Engineering, Massachusetts Institute of Technology, Massachusetts 02139, United States
* To whom correspondence should be addressed: kjh75@hanyang.ac.kr, yslee@snu.ac.kr
† These authors contributed equally to this work.
Electronic Supplementary Information (ESI) available. See DOI: 10.1039/x0xx00000x

of MMP-2.[25, 37-41] One of the common strategies is FRET-based sensing. For instance, the FRET sensors, which employed a fluorescent polymer being complexed with a peptide substrate bearing a quencher through electrostatic force[42] or biotin-protein interaction[43], have been reported for protease detection. These sensing systems, however, suffered from interference by other charged molecules or a lack of direct kinetic measurement for enzyme activity. The other sensing platforms employing quantum dots or upconversion nanoparticles have been reported for protease detection as well[41, 44, 45], however, poor photostability and lower sensitivity need to be addressed. Hence, development of new sensing platforms capable of the sensitive detection of MMP-2 as well as other proteases and the direct measurement of enzyme kinetics is still of great interest.

Herein, we demonstrate a new sensing strategy for the selective detection of MMP-2 secreted from living cells based on the assembly of peptide-functionalized GO, accompanied by self-quenching of its fluorescence. The GO fluorophore was functionalized with a MMP-2 specific peptide substrate bearing a thiol group at the C-terminus to lead to self-assembly of GO via disulfide-bond formation, resulting in the significant amount of self-quenching of GO fluorescence. The peptide-induced GO assemblies were effectively disassembled by proteolytic cleavage of the peptide substrate by MMP-2, which restored the self-quenched GO's fluorescence. Finally, the peptide-induced GO assemblies were successfully applied for the selective detection of MMP-2 secreted by living cells, human hepatocytes HepG2.

2. Experimental

2.1 Chemicals & Materials

Graphite, potassium permanganate ($KMnO_4$), ethanolamine, 1-ethyl-3-(3-dimethylaminopropyl)-carbodiimide (EDC), *N*-hydroxysuccinimide (NHS), dibenzocyclooctyne-PEG_4-acid (DBCO), *N,N*′-diisopropylcarbodiimide (DIC), 4-dimethylaminopyridine (DMAP), anisole, triisopropylsilane (TIPS), 3,6-dioxa-1,8-octanedithiol (DODT), MMP-2 human (recombinant, expressed in E. coli), prinomastat hydrochloride, α-chymotrypsin, and Tris-HCl buffer were purchased from Sigma-Aldrich (St. Louis, MO, USA). Sodium nitrate was purchased from Shimakyu Pure Chemicals (Osaka, Japan). Sulfuric acid, *N,N*′-diisopropylethylamine (DIPEA), *N*-methyl-2-pyrrolidone (NMP), dimethyl sulfoxide (DMSO), methanol, diethyl ether, dichloromethane (DCM), piperidine, dimethylformamide (DMF), hydrogen peroxide, and trifluoroacetic acid (TFA) were purchased from Dae-Jung Chemicals (Siheung, Korea). Rink amide MBHA resin (0.41 mmol/g), Fmoc-protected amino acids, benzotriazole-1-yl-oxy-tris(dimethylamino)phosphonium hexafluorophosphate (BOP), hydroxybenzotriazole (HOBt), 4-hydroxymethyl-2*(5H)*-furanone five-millilitre filtered reactors (Libra tube RT-5M) were purchased from BeadTech Inc. (Seoul, Korea). Azidohexanoic acid was purchased from Novabiochem (Darmstadt, Germany). HepG2 cells were purchased from the Korean Cell Line Bank (Seoul, Korea). Minimum essential medium (MEM) containing 4-(2-hydroxyethyl)-1-piperazineethanesulfonic acid (HEPES) and sodium bicarbonate ($NaHCO_3$); penicillin; heat-inactivated fetal bovine serum (FBS); and 0.25% trypsin–0.53% mM EDTA (0.25% TE) were purchased from Gibco (Carlsbad, CA, USA). Human MMP-2 Enzyme liked immunosorbent assay (ELISA) kit was purchased from Abcam (Cambridge, MA, USA).

2.2 Instruments

Atomic force microscopy (AFM) images were acquired using a scanning probe microscope system (MultiMode 8, Bruker AFM Probes, Camarillo, CA, USA). Fourier transform infrared (FT-IR) spectra were obtained using a FT-IR spectrometer (Nicolet 6700, Thermo Scientific, Waltham, MA, USA). C, H, and N elemental analysis data were acquired using an elemental analyzer (CHNS-932, LECO Inc., St. Joseph, MI, USA). Peptides were synthesized using automatic peptide synthesizer (CS336X, CSBio, Menlo Park, CA, USA). Peptide derivatives were purified using semi-preparative RP-HPLC (Thermo Scientific Spectra System AS3000; Thermo-Fisher, Waltham, MA, USA). Mass spectrometry was carried out using a triple quadrupole tandem mass spectrometer (Quattro, Waters Micromass, Milford, MA, USA). X-ray photoelectron spectroscopy (XPS) experiments were carried out using an AXIS His spectrometer (Kratos Analytical Ltd., Kyoto, Japan). Fluorescence spectra were acquired using a fluorescence spectrometer (LS-55, PerkinElmer, Waltham, MA, USA). Cells were incubated in CO_2 incubator (Sanyo, Osaka, Japan). Absorbance spectra of GO-Peptide were obtained using a UV spectrometer (Optizen 2120UV, Mecasys, Daejeon, Korea). Absorbance for ELISA was read using a microplate spectrophotometer (MQX200R, BioTek Inc., Winooski, VT, USA).

2.3 Preparation of GO-Peptide hybrids

Peptides were synthesized by means of a conventional solid-phase synthesis method. Three different peptide sequences (peptides 1–3) containing a tetra-proline linker either including an MMP-2 specific substrate or non-specific substrate were synthesized on Rink amide MBHA resin (0.41 mmol/g) using an automatic peptide synthesizer. Azidohexanoic acid (2 equiv) was manually introduced to the peptide-anchored resin using BOP (2 equiv), HOBt (2 equiv), and DIPEA (4 equiv) in NMP. The coupling reaction was continued for 2 h at RT and then the completion of coupling reaction was monitored by ninhydrin color test. The resulting azido peptide (N_3-peptide) was separated from the resin by treating it with a cleavage cocktail (TFA/anisole/DODT/TIPS = 95.5/2/1.5/1 (v/v)) for 2 h at RT. The resin was filtered, and the filtrate was concentrated under high vacuum. Finally, cold diethyl ether was added to obtain N_3-peptides as a white powder. These crude N_3-peptides were further purified using semi-preparative RP-HPLC with an A to B gradient (A: 0.1% TFA in water, B: 0.1% TFA in acetonitrile; varied from 10% to 90% B over 30 min, at the flow rate of 4.0 mL/min) and were then freeze-dried. The peptide was identified by triple quadrupole tandem mass spectrometry conducted at the National Instrumentation Center for Environmental Management (NICEM, Seoul, Korea).

View Article Online
DOI: 10.1039/C6NR02815B

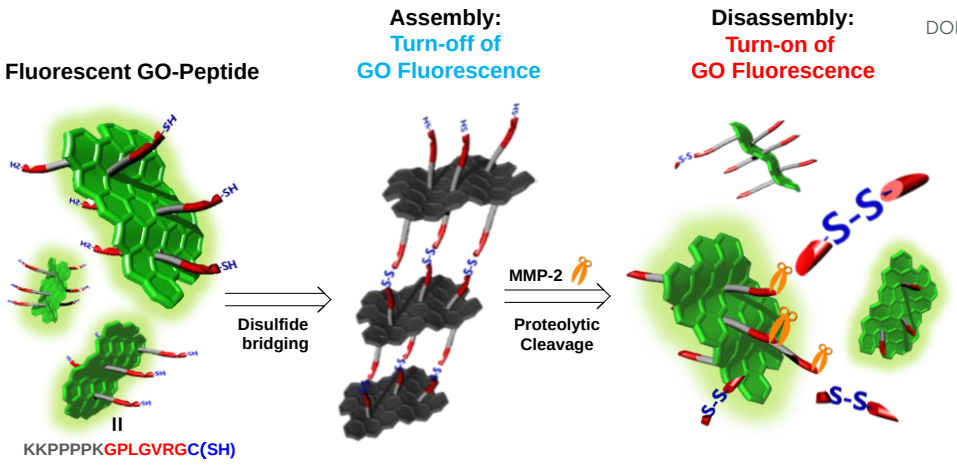

Figure 1. Schematic illustration of peptide-mediated graphene oxide (GO) assembly and its disassembly triggered by proteolytic cleavage for the turn-on fluorescence detection of matrix metalloproteinase-2 (MMP-2).

Graphene oxide (GO) was prepared from graphite flakes using a modified Hummer's method. Graphite was oxidized in H_2SO_4 and $KMnO_4$, and subsequently sonicated for 1.5 h at 12 W in an ice bath. After centrifugation, GO was washed intensively with water. The GO was then reacted with ethanolamine to introduce more surface hydroxyl groups. GO was premixed with EDC (20 equiv) and NHS (20 equiv) in PBS (50 mM, pH 6.0) for 30 min, followed by the addition of ethanolamine (40 equiv), and the coupling reaction was allowed to proceed for 3 h at RT. The resulting hydroxyl-rich ethanolamine–GO (GO-OH) solution was washed with water by centrifugation (13,000 rpm for 10 min) more than three times, and then dialyzed overnight. For use in further reactions, the solvent of the GO-OH solution was exchanged to DMF by centrifugation (15,000 rpm for 40 min) more than three times. DBCO (1.1 equiv) was dissolved in anhydrous DCM. DIC (1.1 equiv) was added and premixed for 30 min. DBCO activated by DIC was added to GO-OH in DMF solution (2 mg/mL) with DMAP (0.1 equiv). The reaction was allowed to proceed for 6 h with vigorous shaking at RT. The DBCO conjugated GO (GO-DBCO) was washed with DMF and water by centrifugation (15,000 rpm for 15 min) multiple times. One and a half milliliters of GO-DBCO aqueous solution (1 mg/mL) was reacted with 0.5 mL of N_3-peptide (1.1 equiv) in PBS (50 mM, pH 7.0) for 2 h with vigorous stirring at RT. The resulting GO–peptide hybrid was washed with water and then dialyzed overnight. Finally, the GO–peptide hybrid was suspended in a mixture of DMSO and water (1:1) with vigorous shaking (1400 rpm) overnight to form disulfide bonds. The suspension was then dialyzed overnight.

2.4 Kinetic measurement of MMP-2 activity over GO-P1 assembly

GO-P1 assembly was diluted with Tris-HCl buffer (50 mM, pH 7.8) to prepare samples with the concentrations of 10, 50, and 100 μg/mL, and subsequently MMP-2 (5 μg/mL) was added to these solutions. During the initial reaction, the reaction was stopped after various intervals by standing at 4 ˚C, and then fluorescence response was measured under 400 nm excitation. The rates of increase in fluorescence of GO-P1 assembly sensors were measured and plotted versus the concentrations of the peptide substrates on the sensors, giving values of K_m and V_{max} for proteolytic activity as the slope and y-intercept of a linear regression to the data of Lineweaver-Burk plot.

2.5 Detection of MMP-2 secreted by living cells

HepG2 cells were cultured to on a 6 well plate in MEM, 25mM HEPES and 25 mM $NaHCO_3$ 90%, FBS 10% and 50 U/mL penicillin at 37 °C in an incubator at 5% CO_2. When the cell confluence reached to 60%, culture medium was replaced with a fresh medium. The cells were incubated for specific time intervals of 12, 24, and 36 h, and then 180 μL of the cell culture supernatant was taken out at each interval to mix with 20 μL of GO-P1 assembly sensor (0.1 mg/mL) for 2 h at 37 °C with gentle shaking. After 2 h, the fluorescence response of the GO-P1 assembly sensor was measured using a fluorescence spectrometer under 400 nm excitation with a 0.01 s exposure time. In addition, the concentration of MMP-2 secreted by the cells was determined using a Human MMP-2 ELISA kit. A 100 μL portion of each standard and a 180 μL portion of the sample were added into human MMP-2–specific antibody-coated wells. After incubation for 3 h at RT with gentle shaking, the solution was completely removed. A 100 μL portion of biotinylated MMP-2 detection antibody was added to each well and incubated for 1 h at RT with gentle shaking. The solution was discarded, and then a 100 μL of HRP-Streptavidin solution was added to each well and allowed to react for 45 min at RT with gentle shaking. The washing step was repeated, and then 100 μL of TMB one-step substrate reagent was added to each well and incubated for 30 min at RT in the dark with gentle shaking. Absorbance was measured at 450 nm using a microplate spectrophotometer immediately after adding 50 μL of stop solution. A new standard curve was generated for each assay, and each sample was assayed in triplicate. Control experiments were also carried out

View Article Online
DOI: 10.1039/C6NR02815B

Table 1. Peptide sequences coupled onto the surface of fluorescent graphene oxide (GO) for the selective detection of matrix metalloproteinase-2 (MMP-2). A blue color and a green color indicate the enzyme recognition sequences for MMP-2 and chymotrypsin, respectively. A red color indicates a cysteine residue responsible for disulfide bonding.

Entry	Target Enzyme	Sequence
Peptide1	**MMP-2**	N_3-Lys-Lys-$(Pro)_4$-Lys-Gly-Pro-Leu-Gly-Val-Arg-Gly-Cys-$CONH_2$
Peptide2	**MMP-2**	N_3-Lys-Lys-$(Pro)_4$-Lys-Gly-Pro-Leu-Gly-Val-Arg-Gly-Ala-$CONH_2$
Peptide3	**Chymotrypsin** (Negative control)	N_3-Lys-Lys-$(Pro)_4$-Lys-Ala-Ala-Pro-Phe-Cys-$CONH_2$

as follows. MMP-2 inhibitor, prinomastat hydrochloride (50 μM), was added to the HepG2 culture medium, and preincubated for 30 min. GO-P1 assembly (0.1 mg/mL) was treated and further incubated for 2 h to allow enzyme reaction. GO-P2 (0.1 mg/mL) was incubated with the same HepG2 cell culture media for 2 h at RT with gentle shaking. Control experiments were also performed in triplicate.

3. Results and Discussion

3.1 Peptide design for MMP-2

The GO assembly was triggered by the formation of disulfide bonds between the peptides anchored on GO, and its disassembly increased fluorescence by proteolytic hydrolysis in the presence of MMP-2. Fluorescent GO sheets were covalently functionalized with the peptides each bearing both an MMP-2 specific substrate and a sulfhydryl group. The GO assembly sensor is schematically illustrated in Figure 1. Three different peptides were rationally designed for GO functionalization as well as for MMP-2 detection (Table 1). Peptide 1 contained an azide group at the N-terminus to allow its introduction to GO via click chemistry, a hydrophilic and stretchable spacer (KKPPPPK), a MMP-2 substrate sequence (GPLGVRGC)[46], and a sulfhydryl group at the C-terminus for disulfide bond formation. Two additional peptides were synthesized for control experiments to demonstrate the necessity of disulfide bonding-induced assembly of GO and its specificity for MMP-2 detection. Peptide 2 had the same MMP-2 substrate sequence as that of the peptide 1, but contained no cysteine at the C-terminus. Due to the absence of cysteine, it was not expected that peptide 2 would induce assembly of GO sheets via disulfide bond formation, and thus, would not induce self-quenching of GO fluorescence. Peptide 3 contained a non-specific substrate sequence for MMP-2 with cysteine at the C-terminus, and is consequently anticipated to induce GO assembly, but not its disassembly by MMP-2. These three peptides were covalently introduced to GO by means of copper-free click chemistry (Scheme S1).

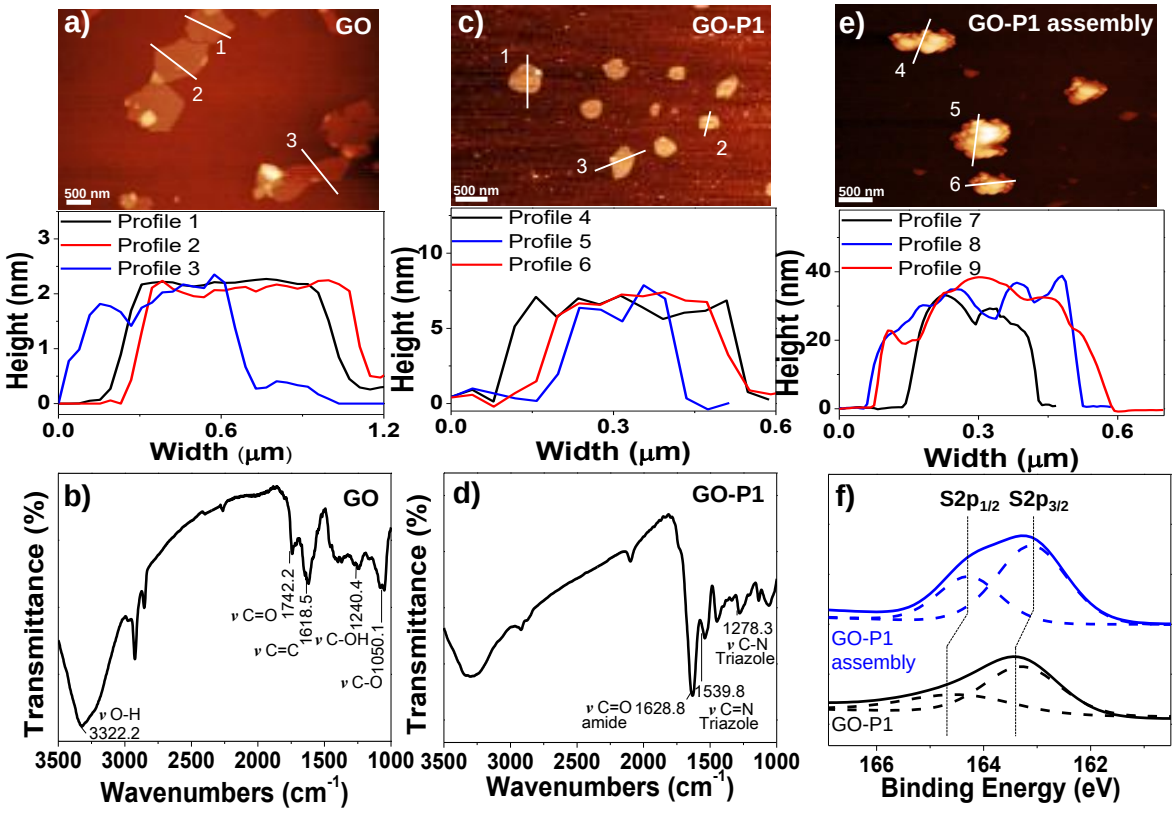

Figure 2. Characterization of GO functionalized with peptide 1 (GO-P1) and its assembly. (a) AFM image and height profile of GO, showing a single sheet of GO of uniform thickness (ca. 2 nm). (b) FT-IR spectrum of GO indicating the presence of various oxygen-containing functional groups. (c) AFM image and height profile of GO-P1 hybrids, showing individually dispersed GO sheets and an increase in their height to 7 nm. (d) FT-IR spectrum of GO-P1 hybrids, showing clear peaks for amide C=O, triazole C=N, and triazole C-N vibrational modes. (e) AFM image and height profile of GO-P1 assembly, showing five or six sheets of GO aggregates and an increase in its height to ca. 37 nm. (f) XPS spectra of GO-P1 hybrids (black line) and GO-P1 assembly (blue line), indicating the formation of disulfide bonds.

View Article Online
DOI: 10.1039/C6NR02815B

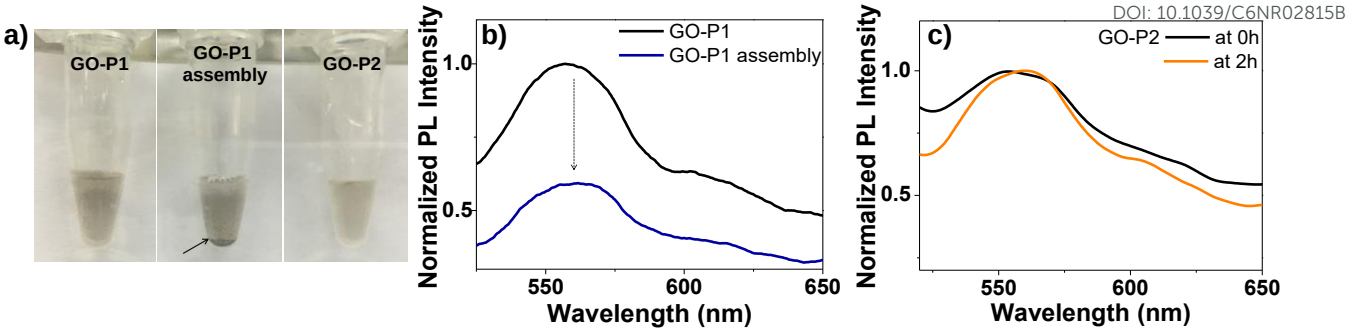

Figure 3. Fluorescence properties of GO-peptide and GO-peptide assemblies. (a) Optical photographs of GO-P1, GO-P1 assembly, and GO-P2 hybrid. A black arrow indicates a precipitated GO-P1 assembly. (b) Fluorescence spectra of GO-P1 (black line) and GO-P1 assembly (blue line), showing the significant fluorescence quenching after assembly. (c) Fluorescence spectra of GO-P2 hybrid at 0 h (black line) and in 2 h (orange line), showing no change in its fluorescence intensity. Fluorescence spectra were normalized by the maximum intensity (560 nm) of GO-P1; all spectra were obtained under excitation at 400 nm.

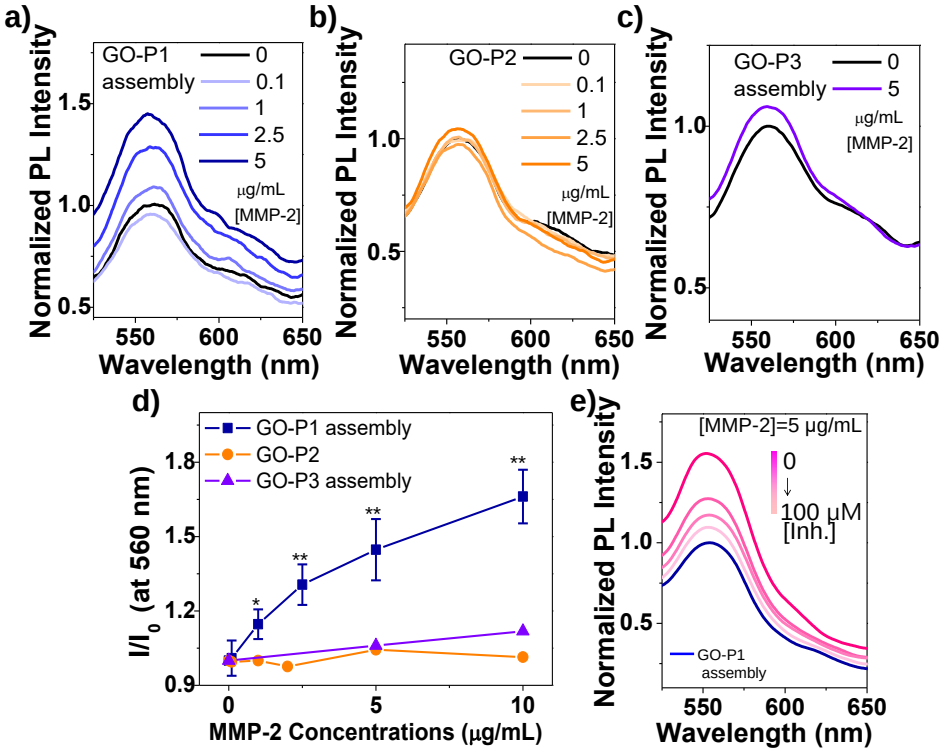

Figure 4. Turn-on fluorescence detection of MMP-2 with GO-peptide assemblies. Fluorescence responses of (a) GO-P1 assembly, (b) GO-P2 hybrid, and (c) GO-P3 assembly to MMP-2 at various concentrations. (d) Fluorescence recovery of GO-P1 assembly, GO-P2 hybrid, and GO-P3 assembly in response to various concentrations of MMP-2; I_0 and I are the intensities at 560 nm in the fluorescence spectra of the sensors before and after addition of MMP-2, respectively. *P<0.05; **P<0.001 (n=3) using one-way ANOVA. (e) Fluorescence response of GO-P1 assembly to MMP-2 (5 μg/mL) in the presence of various concentrations of prinomastat hydrochloride, a MMP-2 inhibitor. All spectra were obtained under excitation at 400 nm.

3.2 GO-Peptide assembly for optical detection of MMP-2

The GO functionalized with peptide 1 (GO-P1) was characterized as below. The atomic force microscopy (AFM) images and height profiles of GO-P1 showed that the pristine GO increased in its height from 2 nm to 7 nm after peptide conjugation, indicating the successful conjugation of the peptide 1 onto the GO surface (Figures 2a and 2c). The structure of GO-P1 was then analyzed further by FT-IR spectroscopy. Vibrational peaks of an amide carbonyl group (C=O 1628 cm^{-1}) and a triazole group (C=N 1539 cm^{-1}, C–N 1278 cm^{-1}) were distinctly detected in the IR spectrum of GO-P1 (Figure 2d) but not in that of pristine GO (Figures 2b), indicating the formation of covalent bonding of peptide 1 to GO. Additionally, the nitrogen content of GO-P1 significantly increased relative to that of pristine GO and to that of DBCO-functionalized GO (Figure S2c), indicating successful conjugation of peptide 1 to GO. Functionalization of GO with the other peptides was also confirmed by the same method used for GO-P1.

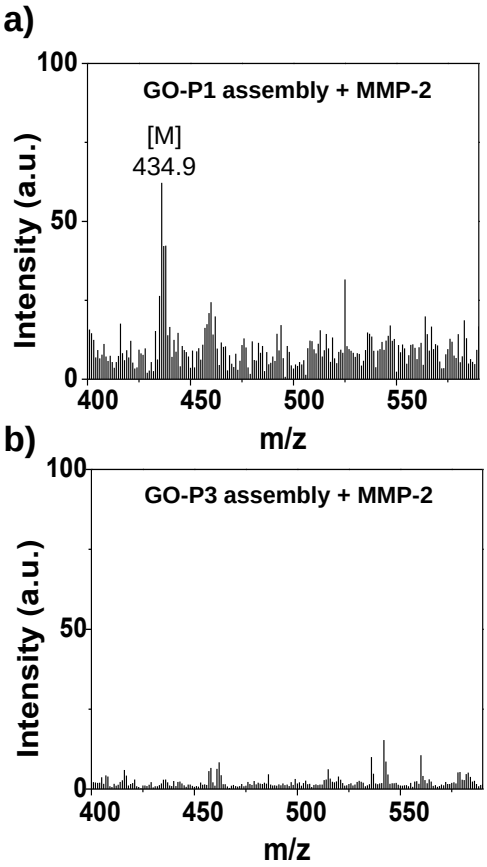

Figure 5. Mass spectrometry analysis of the GO-P1 assembly treated with MMP-2. (a) Mass spectrum of the GO-P1 assembly solution after treatment with MMP-2, showing a peak at 434.9 *m/z*, attributed to the cleaved peptide fragment, VRGC. The calculated mass for $C_{16}H_{34}N_8O_4S$ [M] is 434.5. (b) Mass spectrum of a solution of GO-P3 assembly after MMP-2 treatment, showing no cleaved fragments.

GO-P1 sheets were assembled spontaneously when the GO-P1 dispersion was in DMSO (1 mg/mL) at RT. The resulting GO-P1 assembly was analyzed by AFM (Figure 2e), clearly showed that an aggregated form of GO-P1 assembly increased noticeably its height and lateral size. Its height and width noticeably increased to c.a. 37 nm and c.a. 500 nm, respectively, indicating that each grain was comprised 5 to 7 sheets of GO-P1. The GO-P1 assembly was characterized by XPS (Figure 2f) to investigate whether it was mediated by disulfide bonding of the peptides. The S2p spectrum of GO-P1 before the assembly showed a doublet peak at 163.27 and 164.45 eV with a 2:1 peak area ratio, attributed to $S2p_{3/2}$ and $S2p_{1/2}$ peaks, respectively. The S2p peaks were shifted to the lower binding energy, 163.10 and 164.28 eV, respectively, after formation of GO-P1 assembly, which indicates that the disulfide bonds were formed among GO-P1 sheets.[47, 48] This clearly confirms that GO-P1 assembly was induced by the formation of disulfide bonds among the peptides on GO-P1.

Next, we investigated the optical properties of the GO-P1 assembly. The GO-P1 assembly was settled at the bottom of a container, where it was optically visible (Figure 3a). On the contrary, GO functionalized with peptide 2 (GO-P2) without cysteine did not exhibit assemblage but showed stable dispersion in an aqueous solution. This result indicates that the sulfhydryl moiety of the peptide 1 bound on GO is crucial for the formation of GO-P1 assembly. In addition, the absorbance maximum of GO-P1 assembly was slightly blue-shifted from 210 to 203 nm compared to that of unassembled GO-peptide hybrid, GO-P2, which indicated formation of H-aggregate (Figure S3).[49] As the fluorescence of the GO-P1 assembly and GO-P2 was measured, we found the fluorescence of the GO-P1 assembly was significantly quenched (Figure 3b), whereas that of the GO-P2 dispersion showed constant fluorescence intensity for 2 h without formation of any assembly (Figure 3c). It is evident that assembly of GO induced by cysteine-containing peptides allows the effective modulation of the self-quenching mechanism. Meanwhile, a slight red-shift was observed in the fluorescence emission of GO-P2 after 2 h standing in solution. We speculate that this red-shift might be caused by a change in dielectric environment surrounding GO due to the conformational variation of the peptide on the surface of GO-P2 during incubation.[50, 51]

We then evaluated the performance of the GO-P1 assembly in the detection of MMP-2 activity. The self-quenched fluorescence of the GO-P1 assembly was gradually restored proportional to the MMP-2 concentration (Figures 4a and 4d), but not with chymotrypsin (Figure S4). This is a clear demonstration that the fluorescence restoration was caused specifically by MMP-2, which can be attributed to the proteolytic cleavage of the peptides in the GO-P1 assembly, resulting in its disassembly to individually dispersed GO. On the other hand, the fluorescence of GO-P2, which is incapable of assembly owing to its absence of cysteine, did not respond noticeably to various concentrations of MMP-2 (Figures 4b and 4d). As an additional control, GO was functionalized with peptide 3 (GO-P3), which included cysteine and had a non-specific peptide sequence for MMP-2. The GO-P3 spontaneously assembled, but its self-quenched fluorescence was not restored when MMP-2 was added to the GO-P3 assembly (Figures 4c and 4d), indicating that no enzymatic cleavage of the peptide 3 occurred to in response to MMP-2 due to absence of a specific substrate sequence. Taken together, these results show that the strategy based on GO assembly and disassembly is able to detect MMP-2 activity through its turn-on fluorescence. Hence, the turn-on fluorescence mechanism of GO-P1 can be capitalized as an indicator to determine MMP-2 activity. When a MMP-2 inhibitor was added to the GO-P1 assembly, its turn-on fluorescence response gradually decreased according to the concentration of the inhibitor (Figure 4e). This indicates that the GO-P1 assembly platform can also be applied to the screening of protease inhibitors.

We carried out further analysis to confirm that the disassembly of the GO-P1 assembly was caused by MMP-2 specific proteolysis, which led to the restoration of its self-quenched fluorescence. A solution of the GO-P1 assembly was treated with MMP-2 and measured by means of mass spectrometry (MS) after dithiothreitol (DTT) treatment reducing disulfide bond to completely release the peptide fragments. A peak at m/z = 434.9 in the mass spectrum (Figure 5a and S5a), which is consistent with the mass of the peptide fragment (VRGC-NH_2,

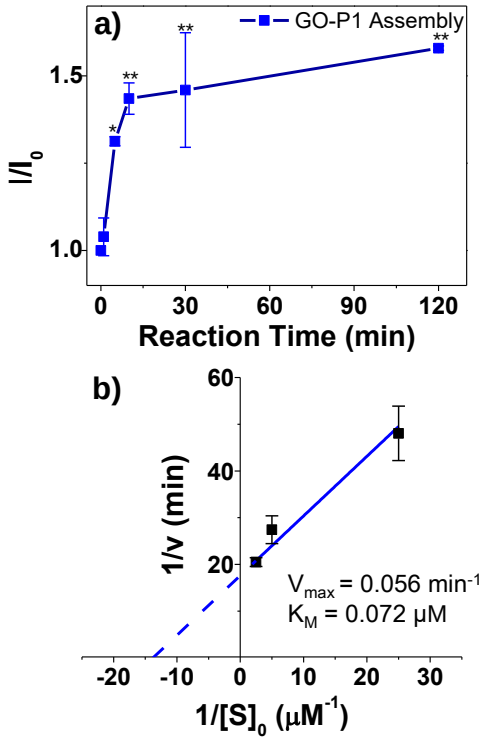

Figure 6. Response kinetics of a GO-P1 assembly for the detection of MMP-2. (a) Turn-on fluorescence response of GO-P1 assembly in response to MMP-2 (5 μg/mL) versus reaction time. *P<0.05; **P<0.01 (n=3) using one-way ANOVA. (b) Lineweaver-Burk plot for the fluorescence response of the GO-P1 assembly sensor to MMP-2 (5 μg/mL); $[S]_0$ is the concentration of GO-P1 assembly, and I_0 and I are the intensities at 560 nm in the fluorescence spectra of the GO-P1 assembly before and after addition of MMP-2, respectively. All spectra were obtained under excitation at 400 nm; all error bars represent standard deviation from the mean values (n = 3).

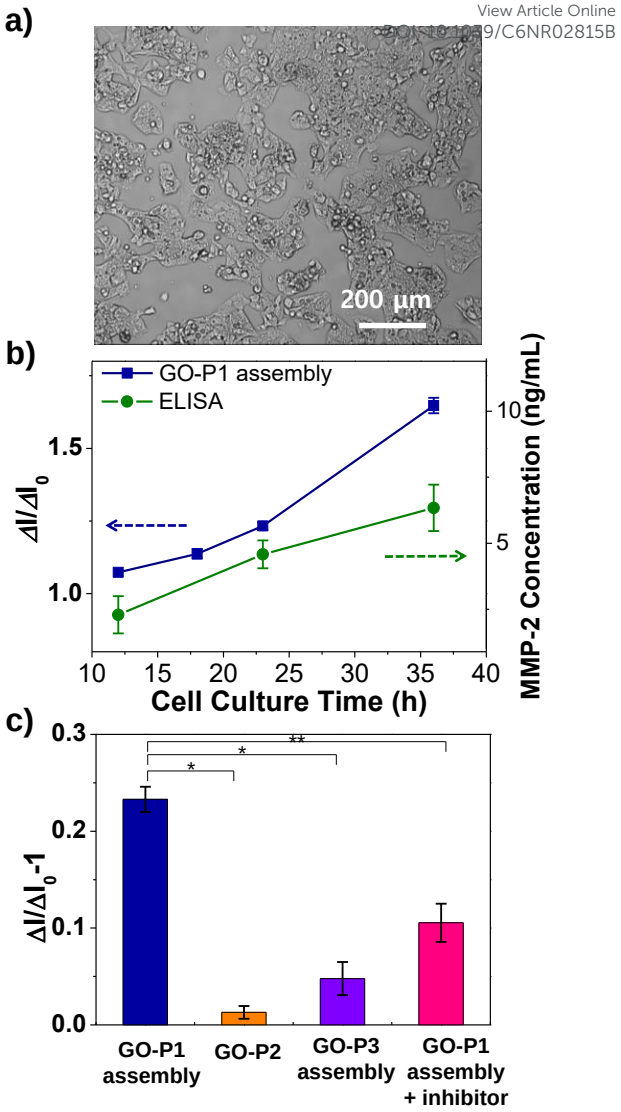

Figure 7. The detection of MMP-2 secreted by living cells with GO-P1 assembly. (a) Optical image of HepG2 cells, (b) Fluorescence response of GO-P1 assembly to cell-secreted MMP-2 (blue line) and ELISA-based quantification of secreted MMP-2 versus cell culture time. (c) Fluorescence recovery of GO-P1 assembly (blue bar), GO-P2 (orange bar), GO-P3 assembly (purple bar), and GO-P1 assembly treated with 50 μM of MMP-2 inhibitor (pink bar) in the media cultured with cells for 24 h. ΔI_0 and ΔI indicate cell media background subtracted fluorescence intensity after incubation of cell-free media and of HepG2 cell-cultured media, respectively. *P<0.001; **P<0.01 (n=3) using one-way ANOVA. All error bars represent standard deviation from the mean.

MW 434.5) hydrolyzed by MMP-2. The peptide fragment (VRGA-NH_2, MW 401.4) from the GO-P2 treated with MMP-2 was also detected in the MS spectrum (Figure S5b, left panel). The MS data of GO-P1 assembly and GO-P2 treated with MMP-2 clearly indicate that peptide substrate was cleaved by MMP-2 regardless of assembly. On the contrary, the MS spectrum of a GO-P3 assembly treated with MMP-2 did not show any specific peak for the cleaved peptide fragment (Figures 5b and S5c, left panel), and no extra mass fragments were observed in the mass spectra of any samples that were not treated with MMP-2 (Figure S5, all right panels). These results provide strong evidence that the GO-P1 assembly was specifically disassembled by MMP-2-triggered peptide cleavage.

3.3 Kinetic measurement of MMP-2 activity over GO-P1 assembly

Subsequently, we investigated the response kinetics of the GO-P1 assembly for MMP-2 detection. The turn-on fluorescence of the GO-P1 assembly increased in its intensity during incubation with MMP-2 and then reached 80% of restoration within 10 min (Figure 6a). Based on this result, the fluorescence increase rates were determined for different concentrations of the GO-P1 assembly, and the Lineweaver-Burk plot was produced to calculate the response kinetic parameters such as Michaelis constant (K_m) and a maximum rate (V_{max}). The values of K_m and V_{max} were 0.072 μM and 0.056 min^{-1}, respectively, which were smaller than previously reported values.[23] This slower response kinetics of the GO-P1 assembly can be ascribed to decreased accessibility of MMP-2 to the peptide substrate sandwiched by GO sheets causing steric hindrance. However, the response kinetics of the GO-P1 assembly is still within an acceptable range of hydrolysis rates as considering MMP-2 hydrolysis of various peptides.[52]

3.4 Detection of MMP-2 secreted from living cells

At last, we applied the GO-P1 assembly to the detection of MMP-2 secreted by HepG2, human liver hepatocellular

View Article Online
DOI: 10.1039/C5NR02845B

carcinoma cells (Figure S6). It was reported that MMP-2 is predominantly expressed in HepG2 cells, and other MMPs such as MMP-1, 7, 9, and 10 are rarely produced.[53,54] ELISA was used to quantify the changes in the amount of MMP-2 secreted by the cells as the incubation time increased. The amount of human MMP-2 secreted from HepG2 cells increased from 2.2 ng/mL at 12 h of incubation time to 6.3 ng/mL at 36 h (Figure 7a). The fluorescence responses of the GO-P1 assembly were also measured at the same time intervals as those of the ELISA. The self-quenched fluorescence of the GO-P1 assembly was gradually restored when the MMP-2 concentration increased during the cell culture, indicating that this GO-P1-assembly sensor was able to detect MMP-2 secreted by the living cells. This turn-on fluorescence response was well correlated with the ELISA measurements of MMP-2 concentration. The limit of detection (LOD) of the GO-P1 assembly sensor for MMP-2 was 2.0 ng/mL. The sensitivity of GO-P1 assembly for MMP-2 detection is comparable with those of other FRET sensors,[23, 25, 41, 55] but it can be more readily prepared since the GO-P1 assembly sensor does not require any quencher molecules that are essential in the FRET systems. In addition, the GO-P1 assembly sensor allows the rapid and simple detection of MMP-2, taking much shorter time at one step, as compared to ELISA, taking 5 h with multiple steps. In particular, GO-P1 assembly is able to provide kinetic parameters for MMP-2 activity. Evidently from these results, GO-P1 assembly sensor promise applications in rapid and simple monitoring of MMP-2 activity.

We performed additional control experiments to demonstrate the specificity of the GO-P1 assembly for MMP-2. No valid turn-on fluorescence response was observed when the GO-P2, which contained MMP-2 specific substrate peptide but did not assemble, was treated with the secreted MMP-2 in HepG2 cultured media (Figure 7b). In addition, there was no significant recovery of the self-quenched fluorescence of the GO-P3 assembly, which did not bear the MMP-2 substrate sequence. Finally, HepG2 cultured media containing MMP-2 was preincubated with 50 μM of prinomastat hydrochloride, a MMP-2 inhibitor, and then added to the GO-P1 assembly. This yielded a substantially decreased response relative to that of GO-P1 without the inhibitor. These cellular experimental results demonstrated that the assembly-disassembly strategy using the peptide-functionalized GO is an effective way to design the biosensors for the selective detection of MMP-2 secreted by the living cells. This novel GO assembly system could be extended to the application of detecting of various biomolecules as well as of high-throughput screening of protease inhibitors.

4. Conclusions

We have developed a GO-peptide assembly sensor in a rapid and simple manner based on spontaneous self-assembling without using additional quencher molecules for MMP-2 detection. The GO assembly and disassembly strategy enabled to generate the fluorescence turn-on sensing platform that was highly selective and sensitive to MMP-2. This GO-peptide assembly sensor was able to report the kinetic parameters in relation to MMP-2 activity as well. Finally, the GO-peptide assembly sensor was capable of the faster and more effective detection of MMP-2 secreted by living cells than the conventional assay. We believe that this sensing principle can be expanded to the detection and monitoring of all other cell-secreted proteases as well as developing their inhibitors.

Acknowledgement

This work was supported by the Basic Science Research Program (NRF-2014R1A2A1A11051877 and 2008-0061891), and by the Pioneer Research Center Program (NRF-2011-0021021) through the National Research Foundation of Korea (NRF) funded by the Ministry of Science, ICT and Future Planning.

Reference

1 N. L. Rosi and C. A. Mirkin, *Chem. Rev.*, 2005, **105**, 1547-1562.
2 S. I. Lim and C. J. Zhong, *Acc. Chem. Res.*, 2009, **42**, 798-808.
3 I. U. Arachchige and S. L. Brock, *Acc. Chem. Res.*, 2007, **40**, 801-809.
4 D. Vanmaekelbergh and P. Liljeroth, *Chem. Soc. Rev.*, 2005, **34**, 299-312.
5 K. Mizusawa, Y. Ishida, Y. Takaoka, M. Miyagawa, S. Tsukiji and I. Hamachi, *J. Am. Chem. Soc.*, 2010, **132**, 7291-+.
6 W. T. Wu, T. Zhou, A. Berliner, P. Banerjee and S. Q. Zhou, *Angew. Chem. Int. Ed.*, 2010, **49**, 6554-6558.
7 J. B. Liu, X. H. Yang, K. M. Wang, R. H. Yang, H. N. Ji, L. Y. Yang and C. L. Wu, *Chem. Commun.*, 2011, **47**, 935-937.
8 T. Kim, M. Noh, H. Lee, S. W. Joo, S. Y. Lee and K. Lee, *J. Phys. Chem. B*, 2009, **113**, 14487-14490.
9 Y. Liu, K. R. Wang, D. S. Guo and B. P. Jiang, *Adv. Funct. Mater.*, 2009, **19**, 2230-2235.
10 Y. Hama, Y. Urano, Y. Koyama, A. J. Gunn, P. L. Choyke and H. Kobayashi, *Clin. Cancer Res.*, 2007, **13**, 6335-6343.
11 Y. Hama, Y. Urano, Y. Koyama, M. Kamiya, M. Bernardo, R. S. Paik, I. S. Shin, C. H. Paik, P. L. Choyke and H. Kobayashi, *Cancer Res.*, 2007, **67**, 2791-2799.
12 H. Kobayashi, M. Ogawa, R. Alford, P. L. Choyke and Y. Urano, *Chem. Rev.*, 2010, **110**, 2620-2640.
13 X. Sun, Z. Liu, K. Welsher, J. T. Robinson, A. Goodwin, S. Zaric and H. Dai, *Nano Res.*, 2008, **1**, 203-212.
14 Z. Luo, P. M. Vora, E. J. Mele, A. C. Johnson and J. M. Kikkawa, *Appl. Phys. Lett.*, 2009, **94**, 111909.
15 G. Eda, Y. Y. Lin, C. Mattevi, H. Yamaguchi, H. A. Chen, I. Chen, C. W. Chen and M. Chhowalla, *Adv. Mater.*, 2010, **22**, 505-509.
16 J. Shang, L. Ma, J. Li, W. Ai, T. Yu and G. G. Gurzadyan, *Sci. Rep.*, 2012, **2**.
17 T. Gokus, R. Nair, A. Bonetti, M. Bohmler, A. Lombardo, K. Novoselov, A. Geim, A. Ferrari and A. Hartschuh, *ACS Nano*, 2009, **3**, 3963-3968.
18 K. P. Loh, Q. L. Bao, G. Eda and M. Chhowalla, *Nat. Chem.*, 2010, **2**, 1015-1024.
19 S. K. Cushing, M. Li, F. Q. Huang and N. Q. Wu, *ACS Nano*, 2014, **8**, 1002-1013.
20 M. Roy, T. S. Kusurkar, S. K. Maurya, S. K. Meena, S. K. Singh, N. Sethy, K. Bhargava, R. K. Sharma, D. Goswami, S. Sarkar and M. Das, *3 Biotech*, 2014, **4**, 67-75.
21 J. H. Jung, D. S. Cheon, F. Liu, K. B. Lee and T. S. Seo, *Angew. Chem. Int. Ed.*, 2010, **49**, 5708-5711.
22 J. L. Chen, X. P. Yan, K. Meng and S. F. Wang, *Anal. Chem.*, 2011, **83**, 8787-8793.
23 S. Y. Kwak, J. K. Yang, S. J. Jeon, H. I. Kim, J. Yim, H. Kang, S. Kyeong, Y. S. Lee and J. H. Kim, *Adv. Funct. Mater.*, 2014, **24**, 5119-5128.

24 S. J. Jeon, S. Y. Kwak, D. Yim, J. M. Ju and J. H. Kim, *J. Am. Chem. Soc.*, 2014, **136**, 10842-10845.
25 D. Feng, Y. Zhang, T. Feng, W. Shi, X. Li and H. Ma, *Chem. Commun.*, 2011, **47**, 10680-10682.
26 M. Zhang, B.-C. Yin, X.-F. Wang and B.-C. Ye, *Chem. Commun.*, 2011, **47**, 2399-2401.
27 H. Jang, Y. K. Kim, H. M. Kwon, W. S. Yeo, D. E. Kim and D. H. Min, *Angew. Chem*., 2010, **122**, 5839-5843.
28 T. Feng, D. Feng, W. Shi, X. Li and H. Ma, *Mol. Biosys.*, 2012, **8**, 1441-1445.
29 M. J. Bissell and D. Radisky, *Nat. Rev. Cancer*, 2001, **1**, 46-54.
30 M. Egeblad and Z. Werb, *Nat. Rev. Cancer*, 2002, **2**, 161-174.
31 M. Nakajima, K. Morikawa, A. Fabra, C. D. Bucana and I. J. Fidler, *J. Natl. Cancer Inst.*, 1990, **82**, 1890-1898.
32 H. Kawamata, S. Kameyama, K. Kawai, Y. Tanaka, L. Nan, D. H. Barch, W. G. Stetler-Stevenson and R. Oyasu, *Int. J. Cancer*, 1995, **63**, 568-575.
33 G. La Rocca, I. Pucci-Minafra, A. Marrazzo, P. Taormina and S. Minafra, *Brit. J. Cancer*, 2004, **90**, 1414-1421.
34 T. Freestone, R. J. Turner, A. Coady, D. J. Higman, R. M. Greenhalgh and J. T. Powell, *Asterioscler. Thomb. Vasc. Biol.*, 1995, **15**, 1145-1151.
35 C. Lombard, J. Saulnier and J. Wallach, *Biochimie*, 2005, **87**, 265-272.
36 U. Pieper-Fürst, U. Kleuser, W. F. Stöcklein, A. Warsinke and F. W. Scheller, *Anal. Biochem.*, 2004, **332**, 160-167.
37 W. J. Akers, B. Xu, H. Lee, G. P. Sudlow, G. B. Fields, S. Achilefu and W. B. Edwards, *Bioconjug. Chem.*, 2012, **23**, 656-663.
38 G. Yang, L. Li, R. K. Rana and J.-J. Zhu, *Carbon*, 2013, **61**, 357-366.
39 J. McIntyre, B. Fingleton, K. Wells, D. Piston, C. Lynch, S. Gautam and L. Matrisian, *Biochem. J.*, 2004, **377**, 617-628.
40 S. Lee, E. J. Cha, K. Park, S. Y. Lee, J. K. Hong, I. C. Sun, S. Y. Kim, K. Choi, I. C. Kwon and K. Kim, *Angew. Chem.*, 2008, **120**, 2846-2849.
41 H. Yao, Y. Zhang, F. Xiao, Z. Xia and J. Rao, *Angew. Chem. Int. Ed.*, 2007, **46**, 4346-4349.
42 M. R. Pinto and K. S. Schanze, *Proc. Natl. Acad. Sci. U.S.A*., 2004, **101**, 7505-7510.
43 S. Kumaraswamy, T. Bergstedt, X. Shi, F. Rininsland, S. Kushon, W. Xia, K. Ley, K. Achyuthan, D. McBranch, and D. Whitten, *Proc. Natl. Acad. Sci. U.S.A*., 2004, **101**, 7511-7515.
44 I. L. Medintz, A. R. Clapp, F. M. Brunel, T. Tiefenbrunn, H. T. Uyeda, E. L. Chang, J. R. Deschamps, P. E. Dawson, and H. Mattoussi, *Nat. Mater*. 2006, **5**, 581-589.
45 Y. Wang, P. Shen, C. Li, Y. Wang, and Z. Lie, *Anal. Chem.*, 2012, **84**, 1466-1473.
46 J. Seltzer, K. Akers, H. Weingarten, G. Grant, D. McCourt and A. Eisen, *J. Biol. Chem.*, 1990, **265**, 20409-20413.
47 C. Wei, M. Chen, J. Tao, X. Wu, M. Khan, D. Liu, N. Huang and L. Li, *Polym. Chem.*, 2014, **5**, 7034-7041.
48 A. L. Vance, T. M. Willey, A. J. Nelson, T. Van Buuren, C. Bostedt, L. J. Terminello, G. A. Fox, M. Engelhard and D. Baer, *Langmuir*, 2002, **18**, 8123-8128.
49 M. Şinoforoğlu, B. Gür, M. Arık, Y. Onganer and K. Meral, *RSC Adv.*, 2013, **3**, 11832-11838.
50 D. A. Heller, E. S. Jeng, T.-K. Yeung, B. M. Martinez, A. E. Moll, J. B. Gastala and M. S. Strano, *Science*, 2006, **311**, 508-511.
51 G. Bisker, J. Dong, H. D. Park, N. M. Iverson, J. Ahn, J. T. Nelson, M. P. Landry, S. Kruss and M. S. Strano, *Nat. Commun.*, 2016, **7**, DOI: 10.1038/ncomms10241.
52 B. E. Turk, L. L. Huang, E. T. Piro and L. C. Cantley, *Nat. Biotech.*, 2001, **19**, 661-667.
53 A. Monvoisin, C. Bisson, K. Si-Tayeb, C. Balabaud, A. Desmoulière and J. Rosenbaum, *Int. J. Cancer*, 2002, **97**, 157-162.
54 T.-W. Chung, S.-K. Moon, Y.-C. Lee, J.-G. Kim, J.-H. Ko and C.-H. Kim, *Arch. Biochem. Biophys.*, 2002, **408**, 147-154.
55 E. Song, D. Cheng, Y. Song, M. Jiang, J. Yu and Y. Wang, *Biosens. Bioelectron.*, 2013, **47**, 445-450.